Characterization of Electronic Displays using CMOS-Compatible Single Photon Avalanche Diode Image Sensors

Characterization of Electronic Displays using CMOS Single Photon Avalanche Diode Image Sensors

Hanning Mai[1], Istvan Gyongy[1], Neale A.W. Dutton[2], Robert K. Henderson[1] and Ian Underwood[1].
[1]School of Engineering, Institute for Integrated Micro and Nano Systems, The University of Edinburgh, Edinburgh, EH9 3JL, UK, Email: h.mai@ed.ac.k
[2]STMicroelectronics Imaging Division, 1 Tanfield, Edinburgh EH3 5DA

Abstract

Advanced CMOS Single Photon Avalanche Diode Array technology is progressing rapidly and is being deployed in a wide range of applications. We report for the first time the use of a CMOS Single Photon Avalanche Diode Array to perform detailed optical measurements on pixels of an OLED microdisplay at very high sampling rate, very low light level and over a very wide dynamic range of luminance. This offers a clear demonstration of the huge potential of this Single Photon Avalanche Diode technology to reveal hitherto obscure details of the optical characteristics of individual and groups of OLED pixels.

I. Introduction

SPADs

The Single-Photon Avalanche Diode (SPAD) was first reported by McIntyre in 1961 [1]. Conceptually, and functionally a SPAD can be thought of as a solid-state analog of a conventional Photo-Multiplier Tube (PMT) [2]. It is a specially designed avalanche photon diode biased above breakdown voltage to operate in Geiger mode, allowing single photon detection. SPADs have been designed and fabricated in a range of technologies from InGaAs-InP [3] and GaN [4] to CMOS [5] that offer a range of performance parameters such as visible and NIR sensitivity. SPAD technologies that utilise a planar substrate allow 2-D arrays of SPADs to be implemented such as [6]. In particular the advent of SPADs that are compatible with fabrication in a mainstream Complementary Metal Oxide Semiconductor (CMOS) process have lowered the barrier to entry via the fabless-design / Multi Product Wafer (MPW) business model. The photosensitive part of a SPAD fabricated in a CMOS process is a silicon p-n junction diode meaning that such SPADs have approximately the same range of wavelength sensitivity as the photodiodes in conventional CMOS image sensors. They are, therefore, quite suitable for the optical characterisation of electronic displays across the visible spectrum.

SPADs and SPAD arrays have addressed a wide range of applications due to the combination of their inherent physical properties – solid state, compact and robustness along with their impressive performance capabilities - very fast response (dead time in the order of nanoseconds[7]), extremely high frame rate, higher than one mega frame per second (fps), single-photon sensitivity and ability to time-stamp the instant of photon capture. CMOS SPAD arrays (referred to here simply as CMOS-SPADs) have opened the door to dense arrays of SPAD pixels with local (in-pixel) circuitry plus sophisticated on-chip signal conditioning and processing [5] that can be custom-designed and thus optimised for any given application. By way of example, recently reported applications of SPADs and SPAD arrays range from time-of-flight three-dimensional (3D) vision [8] and fluorescence lifetime imaging microscopy (FLIM) [9] to imaging of ultrafast physical processes like light-in-flight [10]. The market potential of CMOS-SPADs has grown to the point that many CMOS foundries have developed advanced CMOS processes that are optimised for both CMOS circuits and SPAD detectors, for example [11]. With the recent development of these SPAD-optimised advanced CMOS processes it is becoming possible to overcome some of the limitations of earlier generations of CMOS-SPAD arrays such as low Fill-Factor (FF) and implement high-sensitivity SPAD quantum image sensor (QIS) arrays. Bruschini et al. offer a recent review of CMOS-SPAD sensors [12].

In this manuscript, we report on the use of a state-of-the-art CMOS-SPAD array to optically characterize an array of pixels of an electronic display. We demonstrate that the method can measure very high dynamic range and very fast transient optical response. The measurements are carried out on pixels that form part of an Organic Light Emitting Diode (OLED) microdisplay. Our results illustrate the efficacy of the technology and indicate that the technique is applicable to a much wider range of measurements relevant to displays and other photonic technologies.

Microdisplays

Microdisplays are ultra-miniature display panels [13] designed to be viewed under optical magnification, usually in projection or near-to-eye systems. The combination of emissive-nature, fast response, medium to high luminance and low power consumption makes OLED a favoured candidate for near-to-eye systems. However, it is challenging to evaluate the pixel level optical response of OLED microdisplays. OLED microdisplay pixels are extremely small, usually smaller than 10 µm pitch, often with a low total light output per pixel. Furthermore, the optical switching time of an OLED can be much less than one microsecond [14].

Comparison with other image sensor technologies

High performance image sensors (cameras) have been employed for display metrology, especially for Mura, motion blur measurements where single point sensors cannot be applied [15-17]. Meanwhile, current displays are evolving towards high dynamic range (HDR), high resolution (4k and beyond) and high frame rate (>100Hz). Image sensors with high sensitivity and high frame rate are therefore required for optical characterization of display properties such as dynamic range, gamma curve, flicker, uniformity etc. Traditional CCD (Charge-coupled device), electron multiplying CCD (EMCCD) and CMOS cameras are the leading technologies typically employed. However, these technologies are still limited in frame rate and sensitivity. CMOS-SPADs, as described above, offer the opportunity to measure important properties of some electronic displays that conventional sensors struggle to capture.

Thanks to recent advances in CMOS technology, CMOS SPAD arrays with FF of 50% (with microlens), pixel pitch of 8µm and frame rate of over 10 kilo frames per second (kfps) have been demonstrated [7, 18]. With over 35% quantum efficiency in the visible spectrum, a display measurement platform can be offered based on CMOS-SPAD arrays. In this manuscript, we explore the application of SPAD arrays to display measurements, a challenging area where dynamic range and imaging speed are important, and show that CMOS-SPAD arrays offer advantages over CCD, EMCCD and CMOS technology. Table 1 provides several scientific application camera models' benchmarks in comparison with the SPAD array we employed.

Table 1 Image Sensor Specification Value Comparison

TYPE	CCD	EMCCD	SCMOS	BINARY SPAD
MODEL	Hamamatsu Orca-2[19]	Andor iXon Ultra 897[20]	Hamamatsu ORCA-Flash4.0 V3[21]	SPCImager
FULL WELL CAPACITY (e^-)[1]	80,000	180,000	30,000	1
DYNAMIC RANGE	13,333:1	180,000:1	37,000:1	100,000:1[2]
QUANTUM EFFICIENCY	90%	90%	82%	35% (PDE[3])
FILL FACTOR	N/A	100 %	N/A	26%
PIXEL SIZE	13 µm	16 µm	6.5 µm	8 µm
READ NOISE (e^-)	6	<1	1.4	0
DARK NOISE	0.0005 Hz	0.001 Hz	0.05 Hz	25 Hz

[1] The incident light is digitized by converting photons to electrons (e^-). Full well capacity is the number of electrons that can be stored within the well.

[2] Dynamic range in QIS mode, derived from [7] with exposure time varied from 100ns to 100us.

[3] Photon Detection Efficiency, PDE

OTHER NOISE	N/A	0.0018 Hz CIC[4]	N/A	N/A
NON-UNIFORMITY	N/A	N/A	1% DRNU[5], 0.5% PRNU[6]	2% DRNU, 1% PRNU
FRAME RATE	3 fps	595 fps (256×256 crop mode)	100 fps	>10k fps (binary frames)

II. Experimental Setup

QVGA CMOS SPAD Image Sensor

We have employed a CMOS SPAD image sensor for optical measurements. The Quarter Video Graphics Array (QVGA, 320×240) array image sensor (labelled SPCImager) with 8 μm pixel pitch and 26.8% FF was fabricated in the 130 nm Imaging-CMOS process of ST Microelectronics (Fig. 1 (a) [7]). By employing analogue counting and binary memory circuit, the in-pixel circuitry reduction enables a small pixel pitch and high fill-factor. The image sensor can be operated as single-bit digital readout continuously at a rate of several kilo-frames per second (kfps). Fig. 1(b) shows a schematic of the experiment setup with Olympus BH-2 Microscope.

In binary operation mode, the SPCImager is an example of a fast Quantum Image Sensor. The development of CMOS image sensor, as projected by Fossum et al., is towards QIS with sub-electron read noise, sub-micrometre pixel pitch, multi-megapixel resolution and highly oversampled frame rate [22]. Although QIS pixel state is either 0 (no photon detected) or 1 (at least one photon detected), the sum of these binary values or 'bit-planes' in space and/or time provides a spatio-temporally oversampled grayscale image. As illustrated in Table 1, the dynamic range of SPCImager can extend to 100,000:1 via QIS oversampling.

OLED Microdisplay Test Pixel Array

We have implemented several OLED pixel driver circuits in microdisplay test arrays in ST Micro-electronics 130nm Microdisplay CMOS process [23]. A photomicrograph of a 4×6 test array, with surrounding dummy pixels, is displayed in Fig. 1(c). These arrays are deposited with tandem OLED stacks. The measurements reported here are mainly taken on two types of those pixel driver circuits, i.e. the source follower pixels and the pulse width modulation (PWM) pixels. The source follower (SF) pixels apply bias voltage on the OLED. Fig. 1(d) shows the method of generating grayscale for the SF pixels. There are two modes to drive the PWM pixel. It can be operated as an analogue PWM pixel, in which the in-pixel stored voltage is compared with a ramp signal, producing an OLED drive pulse of controlled duration. Or it can be driven as pulse code modulation (PCM) pixel as shown in Fig. 1(e). The in-pixel memory is effectively a 1-bit Dynamic Random-Access Memory (DRAM). The OLED anode voltage is switching between VSS (Low) and VDD (High) by comparing the voltage stored in the DRAM

[4] Clock Induced Charge, CIC

[5] Dark Rate Non-Uniformity, DRNU

[6] Photon Response Non-Uniformity, PRNU

with a static voltage. The source-follower pixels are 4.7µm pixel pitch, and the PWM pixels are 5.2µm pitch.

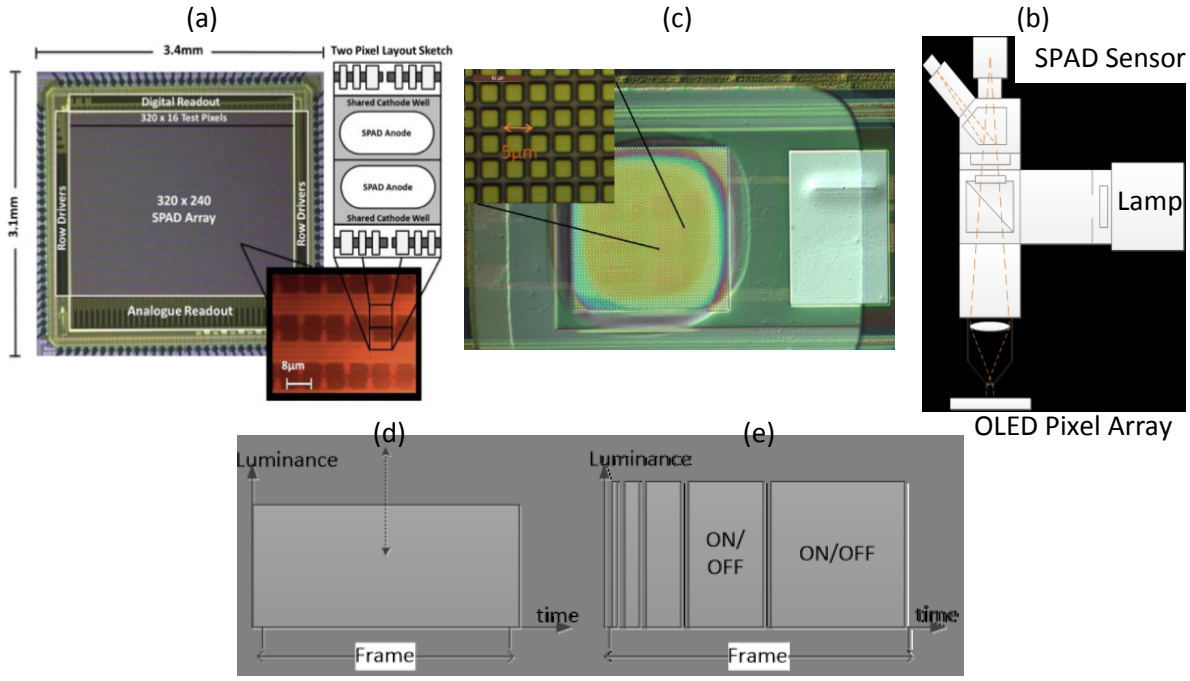

Fig. 1*. (a) Photomicrograph of the SPAD-based QVGA imager [7]. (b) Schematic of the measurement setup based on Olympus BH-2 Microscope. (c) Photomicrograph of test array. Inset: zoom in layout of the 4×6 array with dummy pixels. (d) Grey scale generation for source follower pixel. (e) Grey scale generation for PCM pixel.*

We now describe in detail two very different measurements that we have made that illustrate some of the capabilities of CMOS SPAD arrays for measuring the optical properties of electronic displays. In the first case we measure the light emitted by a single microdisplay pixel. The pixel circuit is that of a conventional two-MOSFET (2T) source-follower and we measure the light emitted as a function of input voltage in a quasi-steady-state scenario. In the second case we measure the fast transient response in order to determine non-idealities in the relative luminance of the different bit-planes in a pixel driven in digital pulse coded modulation mode.

High Dynamic Range Steady State Measurement - Source Follower Pixel

The circuit schematic of the conventional 2T source-follower pixel circuit of the OLED microdisplay is shown in Fig. 2 (a). The drive transistor, MN2, is biased as a source-follower. Thus, in the steady state the OLED anode voltage is $V_{Anode} \cong V_{data} - V_{th}$. By sweeping V_{data}, the output light level of the OLED microdisplay pixel can vary from ~0 photons to >10^6 photons per second.

For SPAD QIS cameras, every "frame" is, in fact, a "bit-plane" in which each pixel has a binary value of 0 (no photon detected) or 1 (*at least* one photon detected). These bit-planes can be summed spatially and/or temporally to generate an "image" with the potential for high dynamic range.

The probability of photons arriving at each SPAD pixel follows a Poisson distribution, i.e. for a time interval of τ, the probability $P[k]$ of k photons arriving is

$$P[k] = \frac{e^{-\phi\tau}(\phi\tau)^k}{k!}.$$

where ϕ is the average photon arrival rate in τ.

Therefore, the probability of no photons arriving is

$$P\,[0] = e^{-\phi\tau},$$

and the probability of at least one photon being detected is

$$P\,[k > 0] = 1 - e^{-\phi\tau}.$$

For a spatial and temporal average of photon count rate (bit density), $E(C_{signal})$,

$$E\left(C_{Signal}\right) = D = 1 - e^{-\phi \cdot FF \cdot PDP \cdot \tau},$$

where the SPAD array's photon detection probability is given by PDP and its fill factor by FF.

For every frame captured, there are photon counts that are a consequence of the dark noise (also called thermal noise or after-pulsing). Thus, the measured photon count bit density is

$$E(C_{measure}) = E\left(C_{signal+noise}\right) = 1 - e^{-(\phi \cdot FF \cdot PDP + DCR)\cdot \tau}.$$

With "hot pixels[7]" removed, the dark count rate (DCR) of the remaining pixels approximates to a Poisson distribution [24]. The dark noise can be removed by simply capturing another background frame, the average photon arrival rate H, in the interval of τ, is shown as follows

$$H_{signal} = \phi \cdot FF \cdot PDP = \frac{1}{\tau}\log\left(\frac{1-E\left(C_{background}\right)}{1-E\left(C_{signal+noise}\right)}\right). \quad (1)$$

By temporal and/or spatial oversampling, the arrival rate of incident photons on SPAD pixels can be recovered from analysis using Poisson arrival statistics[25].

In capturing the image shown in Fig. 2(b), each OLED SF pixel (4.7µm pixel pitch) is optically mapped onto approximately 400 (20×20) SPAD pixels. The incident number of photons is the derivation from the temporal and spatial average photon rate with Equation (1). Fig. 2(c) shows the sweep of V_{data} versus the incident photon counts and pixel current with 100µs exposure time. The incident photon count is derived from 1000× temporal oversampling and 400 spatial binning. The average OLED current per pixel is determined from the measured cathode current of the array divided by the number of pixels. The photon rate versus DATA voltage of two pixels (Pixel 1 located in the blue square, Pixel 2 located in the red square in Fig. 2(b)) is plotted. Similar luminance with small mismatch across different DATA voltage can be found between two pixels.

[7] "Hot pixels" are malfunctioning pixels that demonstrate abnormally high dark count. They are typically defined as those pixels giving more than 5,000 dark counts per second.

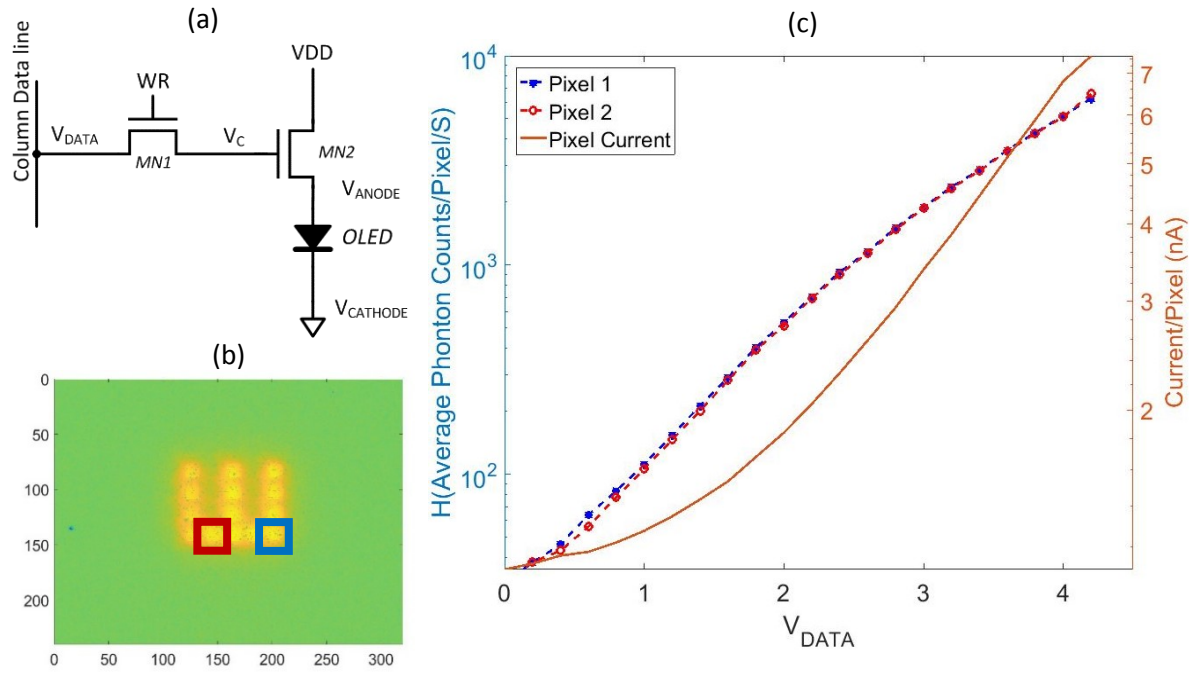

Fig. 2. (a) Source follower circuit schematic. (b) SPAD image of OLED pixel array (1000 oversampled field). (c) Average incident photon rate 1000 oversampled field with 100 μs exposure (left y-axis), average OLED pixel current (right y-axis) vs DATA voltage (x-axis). Pixel 1 (blue asterisk marker) locates in the blue square and Pixel 2 (red circle marker) locates in the red square in (b).

Fast Transient Measurement – Modelling PCM Pixel Optical Response

Another method of achieving grey scale is Pulse-Coded Modulation (PCM). Viewing imperceptibly-fast binary (ON/OFF) switching of the OLED produces the visual impression of grey scale at each pixel. The perceived grey scale is, theoretically, proportional to the on/off time ratio of each frame provided the luminance level is constant during each pulse and from pulse to pulse.

For transient measurement, an 8-bit, 100Hz PCM scheme is applied to the OLED pixel array. The oversampling technique is performed over a period (e.g. the photon counts at t_0 is averaged with t_0+T, where T is the OLED frame time, 10ms). In a similar manner to the steady sate measurement shown in Fig. 2(b), the OLED pixel array is imaged onto the SPCImager. Each OLED PCM pixel (5.2μm pixel pitch) is mapped onto approx. 484 (22×22) SPAD pixels. The pixels are measured at 50kHz (10μs exposure, 10μs readout) frame rate.

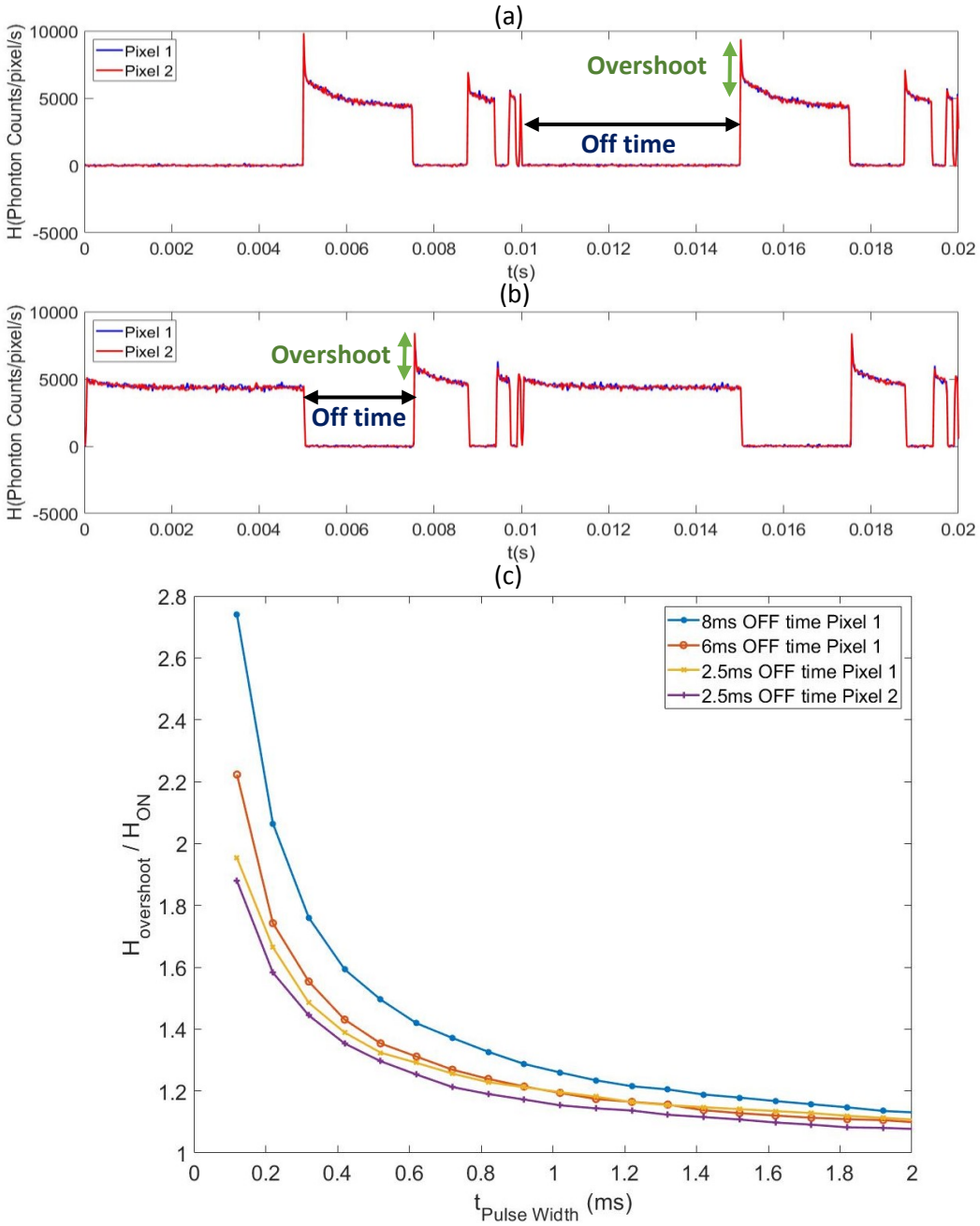

Fig. 3. PCM pixel transient measurement of 100 oversampled field, 484 spatial binning (a) encode 8'b10101010 and (b) encode 8' b01010101 of pixel 1 (blue), pixel 2 (red). (c) Ratio of overshoot versus pulse width with OFF time of 8ms (blue asterisk), 6ms (orange circle) and 2.5ms (yellow cross) of pixel 1 and 2.5ms OFF time of pixel 2 (purple plus sign).

The transient photon counts measurement of two pixels are presented in Fig. 3(a) of 8b'10101010 and Fig. 3(b) 8b'01010101 PCM scheme. The number of photon counts/pixel/s is reconstructed through oversampling 100× temporal oversampling and 484 spatial binning. The two pixels are with similar transient response, small discrepancies are found at the turn-on overshoot level.

We find that the OLED pixel luminance is not constant during each coded pulse. Overshoot and decay behaviour is shown when the pixel is switched ON from OFF. There are several factors that could contribute to the turn-on overshoot in OLEDs, for example, transient charge imbalance[26, 27], recombination of pre-trapped charges[28], and singlet–triplet quenching[29]. The turn-on overshoot happens usually in the scale of microsecond, then settles to the constant level. It is likely to go undetected by measurement systems with measurement time slower than one millisecond.

To quantify the amount of overshoot, we take the integration photons of each pulse ($H_{overshoot}$) and divide it with the photon number of the pixel that is set ON over a full frame (H_{ON}). In this case, the OLED pixel drives a constant ON voltage, it doesn't show any turn-on overshoot behaviour. In Fig. 3(c), the ratio of overshoot to signal is plotted versus different pulse widths with 8ms, 6ms, 2.5ms OFF time of pixel 1 and 2.5ms OFF time of pixel 2. The shorter is the pulse, the more is the luminance deviation. Moreover, the longer the OLED pixel is OFF before it is switched ON, the greater is the luminance overshoot. While the transient responses of pixel 1 and pixel 2 with the same OFF time are similar, any small variation in the overshoot level would cause considerable luminance mismatch at short pulse width.

III. Conclusion

We have demonstrated a novel OLED microdisplay optical characterization method with a SPAD image sensor. SPAD image sensors are expected to match or even exceed the performance of sCMOS and EMCCD for very low light molecule identification[30]. The SPAD image sensors are also capable of observing dynamic behaviour occurring over a very short-time scale[30], (in the present case, OLED pixel luminance overshoot during switch ON) which is inaccessible to most sCMOS sensors. Each SPCImager SPAD pixel can achieve 10^7 photon counts per second for 100ns exposure, and dark count as low as 4 counts/s when cooled, a similar level of performance to that of the PMT single-point sensor reported by Fatadin et al.[31]. Table 2 shows an outline comparison of the SPAD-based SPCImager and other state-of-the-art systems. SPCImager measures significantly faster and is capable of nonuniformity measurement.

When set beside the other technologies of Table 2, CMOS SPAD is a relatively young technology. The commercial potential across a large and diverse range of applications from medical imaging to automotive LIDAR means that CMOS SPAD sensors and arrays are currently the focus of a great deal of research and development effort in both technology and design and are expected to remain so for some years to come. One recent *technology* trend that illustrates this is the development of SPAD-optimized CMOS processes, from Back Side Illuminated (BSI) [32] to 3D stacking [33]. This means that the rate of performance improvement in CMOS SPADs is currently very high and is further enhanced by *design* because Application Specific SPAD ICs – optimally designed for a given application – are readily achievable. Thus, we can look forward to continuing rapid performance improvement in CMOS SPAD arrays that is likely to outpace improvements in the rival technologies.

Table 2 Performance Comparison of SPCImager with existing systems

Measurement system	Image sensor technology	Dynamic range	Minimum Measurement time
SPCImager	SPAD	4 – 10^7 photon counts/s (aprox. 2×10^{-4} – 550 cd/m^2 at 520 nm) for 100ns exposure to 1s exposure, -5C° cooled	5µs including readout for 10×320 of SPAD pixels
2-in-1 Imaging Colorimeter [15]	CMOS	0.01 cd/m^2 – 5000 cd/m^2	65 ms at 100 cd/m^2, 330 ms at 1 cd/m^2
MotionMaster [34]	CCD	N/A - Detects motion blur (Image difference)	typ. 0.26ms – 0.52ms
NPL PMT Spectro-radiometer [31]	PMT	10 – 10^7 photon counts/s[1]	N/A
GLRT Gray Level Response Time Measurement Kit [35] (Hamamatsu H10722-110)	PMT	16-bit DATA	2 µs

IV. Acknowledgements

This work was carried out within the Pilot Optical Line for Imaging and Sensing (POLIS, Project ID 621200) under funding scheme JTI-CP-ENIAC of FP7. The authors appreciate the support from STMicroelectronics who fabricated the SPCImager. We gratefully acknowledge the support and assistance of Michael Thomschke, Sebastien Guillamet of MicroOLED S.A., Benoit Racine of CEA/LETI and Andrew Bunting of University of Edinburgh in the design, fabrication and packaging of the OLED microdisplays and the assistance of Tarek Al Abbas with the SPAD measurements. Hanning Mai is grateful to the China Scholarships Council for University of Edinburgh Scholarship.

V. Reference

[1] R. McIntyre, "Theory of microplasma instability in silicon," *Journal of Applied Physics,* vol. 32, no. 6, pp. 983-995, 1961.

[2] D. Tyndall *et al.*, "A High-Throughput Time-Resolved Mini-Silicon Photomultiplier With Embedded Fluorescence Lifetime Estimation in 0.13 µm CMOS," *IEEE Transactions on Biomedical Circuits and Systems,* vol. 6, no. 6, pp. 562-570, 2012.

[3] S. Pellegrini *et al.*, "Design and performance of an InGaAs-InP single-photon avalanche diode detector," *IEEE Journal of Quantum Electronics,* vol. 42, no. 4, pp. 397-403, 2006.

[4] K. A. Mclntosh *et al.*, "Arrays of III-V semiconductor Geiger-mode avalanche photodiodes," in *The 16th Annual Meeting of the IEEE Lasers and Electro-Optics Society, 2003. LEOS 2003.*, 2003, vol. 2, pp. 686-687 vol.2.

[5] A. Rochas *et al.*, "Single photon detector fabricated in a complementary metal–oxide–semiconductor high-voltage technology," *Review of Scientific Instruments,* vol. 74, no. 7, pp. 3263-3270, 2003.

[6] J. Richardson *et al.*, "A 32x32 50ps resolution 10 bit time to digital converter array in 130nm CMOS for time correlated imaging," in *2009 IEEE Custom Integrated Circuits Conference*, 2009, pp. 77-80.

[7] N. A. Dutton *et al.*, "A SPAD-based QVGA image sensor for single-photon counting and quanta imaging," *IEEE Transactions on Electron Devices,* vol. 63, no. 1, pp. 189-196, 2016.

[8] R. J. Walker, J. A. Richardson, and R. K. Henderson, "A 128×96 pixel event-driven phase-domain ΔΣ-based fully digital 3D camera in 0.13µm CMOS imaging technology," in *2011 IEEE International Solid-State Circuits Conference*, 2011, pp. 410-412.

[9] S. P. Poland *et al.*, "New high-speed centre of mass method incorporating background subtraction for accurate determination of fluorescence lifetime," *Optics express,* vol. 24, no. 7, pp. 6899-6915, 2016.
[10] G. Gariepy *et al.*, "Single-photon sensitive light-in-fight imaging," *Nature communications,* vol. 6, p. 6021, 2015.
[11] *Imaging Premium Foundry, STMicroelectronics*. Available: http://www.st.com/content/st_com/en/about/innovation---technology/imaging.html
[12] C. Bruschini, H. Homulle, and E. Charbon, "Ten years of biophotonics single-photon SPAD imager applications: retrospective and outlook," in *SPIE BiOS*, 2017, vol. 10069, p. 21: SPIE.
[13] I. Underwood, "Introduction to Microdisplays," in *Handbook of Visual Display Technology*, J. Chen, W. Cranton, and M. Fihn, Eds. Berlin, Heidelberg: Springer Berlin Heidelberg, 2012, pp. 2033-2041.
[14] D. Braun, D. Moses, C. Zhang, and A. Heeger, "Nanosecond transient electroluminescence from polymer light‐emitting diodes," *Applied physics letters,* vol. 61, no. 26, pp. 3092-3094, 1992.
[15] M. Wolf and J. Neumeier, "72‐2: A High‐Speed 2‐in‐1 Imaging Colorimeter for Display Production Applications," in *SID Symposium Digest of Technical Papers*, 2016, vol. 47, no. 1, pp. 974-977: Wiley Online Library.
[16] M. E. Becker, T. Fink, and U. Krüger, "29-4: Image Blurring Induced by Scattering Anti-Glare Layers," *SID Symposium Digest of Technical Papers,* vol. 47, no. 1, pp. 372-375, 2016.
[17] H. Jamleh *et al.*, "50.2: Mura Detection Automation in LCD Panels by Thresholding Fused Normalized Gradient and Second Derivative Responses," *SID Symposium Digest of Technical Papers,* vol. 41, no. 1, pp. 746-749, 2010.
[18] I. Gyongy *et al.*, "Cylindrical microlensing for enhanced collection efficiency of small pixel SPAD arrays in single-molecule localisation microscopy," *Optics Express,* vol. 26, no. 3, pp. 2280-2291, 2018/02/05 2018.
[19] *ORCA Ⅱ Digital CCD camera C11090-22B*. Available: http://camera.hamamatsu.com/us/en/product/search/C11090-22B/index.html
[20] *iXon EMCCD Cameras*. Available: http://www.andor.com/cameras/ixon-emccd-camera-series
[21] *ORCA-Flash4.0 V3 Digital CMOS camera*. Available: https://www.hamamatsu.com/jp/en/C13440-20CU.html#1328482115153
[22] E. R. Fossum, "What to do with sub-diffraction-limit (SDL) pixels?—A proposal for a gigapixel digital film sensor (DFS)," in *IEEE Workshop on Charge-Coupled Devices and Advanced Image Sensors*, 2005, pp. 214-217.
[23] H. Mai, R. Henderson, and I. Underwood, "Pixel Drive Circuit Design for AMOLED Microdisplays," in *Eurodisplay*, Berlin, 2017, vol. 1, no. 1, pp. 32-33.
[24] I. M. Antolovic, S. Burri, R. A. Hoebe, Y. Maruyama, C. Bruschini, and E. Charbon, "Photon-counting arrays for time-resolved imaging," *Sensors,* vol. 16, no. 7, p. 1005, 2016.
[25] E. R. Fossum, "Modeling the performance of single-bit and multi-bit quanta image sensors," *IEEE Journal of the Electron Devices Society,* vol. 1, no. 9, pp. 166-174, 2013.
[26] B. Ruhstaller, T. Beierlein, H. Riel, S. Karg, J. C. Scott, and W. Riess, "Simulating electronic and optical processes in multilayer organic light-emitting devices," *IEEE Journal of Selected Topics in Quantum Electronics,* vol. 9, no. 3, pp. 723-731, 2003.
[27] L. Hassine, H. Bouchriha, J. Roussel, and J. L. Fave, "Transient response of a bilayer organic electroluminescent diode: Experimental and theoretical study of electroluminescence onset," *Applied Physics Letters,* vol. 78, no. 8, pp. 1053-1055, 2001/02/19 2001.
[28] C. W. Ma, O. Lengyel, J. Kovac, I. Bello, C. S. Lee, and S. T. Lee, "Time-resolved transient electroluminescence measurements of emission from DCM-doped Alq3 layers," *Chemical Physics Letters,* vol. 397, no. 1, pp. 87-90, 2004/10/11/ 2004.

[29] Y. Zhang, M. Whited, M. E. Thompson, and S. R. Forrest, "Singlet–triplet quenching in high intensity fluorescent organic light emitting diodes," *Chemical Physics Letters,* vol. 495, no. 4, pp. 161-165, 2010/08/10/ 2010.

[30] I. Gyongy *et al.*, "Bit-plane processing techniques for low-light, high speed imaging with a SPAD-based QIS," in *International Image Sensor Workshop, Vaals, The Netherlands*, 2015, pp. 8-11.

[31] I. Fatadin, C. Wall, and K. Vassie, "High - accuracy system for spectral measurement of small - area - contrast and low - light - level display screens," *Journal of the Society for Information Display,* vol. 14, no. 11, pp. 967-971, 2006.

[32] E. Charbon, M. Scandini, J. M. Pavia, and M. Wolf, "A dual backside-illuminated 800-cell multi-channel digital SiPM with 100 TDCs in 130nm 3D IC technology," in *2014 IEEE Nuclear Science Symposium and Medical Imaging Conference (NSS/MIC)*, 2014, pp. 1-4.

[33] T. A. Abbas, N. A. W. Dutton, O. Almer, S. Pellegrini, Y. Henrion, and R. K. Henderson, "Backside illuminated SPAD image sensor with 7.83µm pitch in 3D-stacked CMOS technology," in *2016 IEEE International Electron Devices Meeting (IEDM)*, 2016, pp. 8.1.1-8.1.4.

[34] K. P. Jokinen and W. Nivala, "65 - 4: Novel Methods for Measuring VR/AR Performance Factors from OLED/LCD," in *SID Symposium Digest of Technical Papers*, 2017, vol. 48, no. 1, pp. 961-964: Wiley Online Library.

[35] *Gray Level Response Time Measurement Kit, Westar Display Technologies Inc.* Available: http://www.westardisplaytechnologies.com/products/gray-level-response-time-measurement-kit-glrt/